Optimizing the Vertebrate Vestibular Semicircular Canal: Could We Balance Any Better?

Todd M. Squires

Department of Physics and Department of Applied and Computational Mathematics, California Institute of Technology 114-36, Pasadena, California 91125, USA

(Received 16 January 2004; published 5 November 2004)

The fluid-filled semicircular canals (SCCs) of the vestibular system are used by all vertebrates to sense angular rotation. Despite masses spanning seven decades, all mammalian SCCs are nearly the same size. We propose that the SCC represents a sensory organ that evolution has "optimally designed." Four geometric parameters characterize the SCC, and "building materials" of given physical properties are assumed. Identifying physical and physiological constraints on SCC operation, we find the most sensitive SCC has dimensions consistent with available data. Since natural selection involves optimization, this approach may find broader use in understanding biological structures.

DOI: 10.1103/PhysRevLett.93.198106 PACS numbers: 87.19.Rr, 47.85.–g, 87.19.Bb

Simple physical principles and scaling arguments have been remarkably effective in understanding organismic and evolutionary properties of the animal kingdom [1]. Sensory organs, which transduce physical stimuli into neural signals, are particularly well suited for physical analysis. The biophysics of the cochlea, for example, has been the focus of much recent study [2].

Here we focus on a different inner-ear organ: the fluid-filled semicircular canals (SCCs) that each of the roughly 45 000 vertebrate species employs to mechanically sense rotation [3,4]. Rotation sensation is imperative for balance, but plays an equally important role in vision. The neural output of the SCCs feeds directly to the oculomotor system, causing a reflexive motion of the eyes that compensates for head motion. This allows you to read this article even while shaking your head, which would be much more difficult if the article itself were shaken.

Previously, we studied "top-shelf vertigo," a mechanical disorder of the human SCC [5]. Here, we address a rather astonishing fact: the SCCs of every mammal, from mice to whales, are essentially the same size (Fig. 1) [6,7]. Mammals span seven decades in mass and almost three in length, yet SCC dimensions are restricted to less than one. In fact, the SCC of the human fetus reaches its full adult size by the 14th week of pregnancy [8]. Fish, reptile, amphibian, and bird SCCs are of similar size [6], the one apparent exception being sharks (discussed below) [7]. In exploring reasons for the constancy of cell size, Vogel writes, "anything biological that does not vary in size ought to strike us as noteworthy" [1]. Similarly, SCC nonscaling suggests that these particular dimensions may be special to, and perhaps optimal for, their function.

The idea that biological structures are "optimal" has recently found rather dramatic support. Microcavities in the brittle star skeleton act as perfect lenses [9], and sea sponges develop single-mode optical fibers that rival current technology [10]. The human visual system operates at the single-photon level [11], and the auditory system is limited by thermal noise [12]. In fact, evolution can be viewed as a gradient search seeking to optimize "fitness"; however, the utility of this approach is often limited by the difficulty of defining fitness. By contrast, the semicircular canals have a well-defined purpose, and reasonable measures of their quality can be proposed.

Herein, we suggest that the "universal" size of the SCCs can be understood in terms of a system which has been "optimally designed" by evolution. Others have examined the relation between SCC sensitivity and geometry from a purely fluid standpoint [6,7], but ignored the elastic membrane and sensory hair cells that complete the transduction process, and which depend on SCC dimensions. Our approach is as follows: we start with SCC "blueprints" without dimensions (Fig. 2), and assume basic building materials (solid walls, fluid endolymph, elastic material, and hair cells) to be given. Identifying physically and physiologically reasonable constraints, we find a unique set of well-constrained and robust optimal

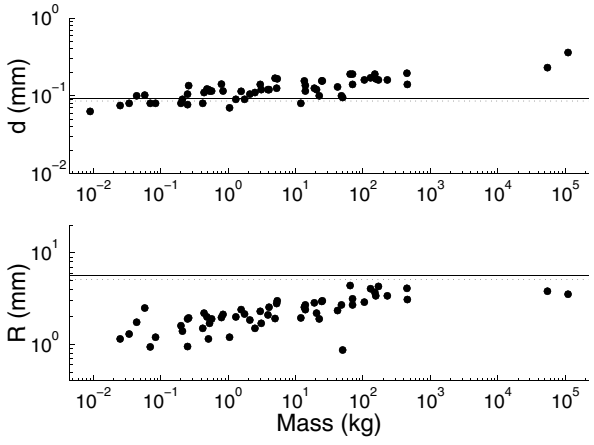

FIG. 1. Measured values of R and d for mammals [6,7]. Despite seven decades of mass variation, variations in R and d are limited to about one decade. Solid (dashed) horizontal lines reflect optimal (tolerant) SCC dimensions (12)–(15). Rough measurements of c and t for mammals [25] reveal $t \sim 0.15$–0.44 mm and $c \sim 0.17$–0.5 mm (cf. optimal $c = 0.12$ and $t = 0.12$).

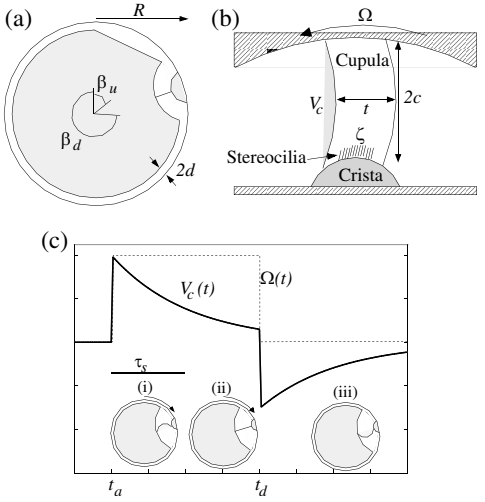

FIG. 2. (a) The semicircular canal is a torus of major radius R, with a long narrow duct of radius d spanning an angle β_d. (b) The ampulla contains an elastic cupula of thickness t and radius c, which distorts under SCC rotation, causing embedded hair cell stereocilia to deflect a distance ζ and trigger a neural signal. Measured values (in mm) for humans are $\{R_h, c_h, d_h, t_h\} = \{2.8, 0.44, 0.19, 0.31\}$ [25]. (c) SCC operation: (i) Angular velocity is impulsively accelerated to Ω_0 at t_a and the cupula distorts by $V_c \propto \Omega_0$. (ii) Under sustained rotation, the cupula relaxes and forgets Ω_0. (iii) Upon decelerating to rest at t_d, fluid inertia causes a (negative) cupular displacement, eliciting dizziness.

dimensions that maximize SCC sensitivity. Moreover, they are consistent with measured data (Fig. 1).

We begin with a description of basic SCC structure (Fig. 2). Each ear contains three mutually orthogonal SCCs to span the three rotation axes. Each SCC is a hollow torus of major radius R that consists of a narrow *duct* of radius d and a bulbous *ampulla* of radius c, all filled with waterlike *endolymph* of density ρ and viscosity μ. The *cupula*, a mucus membrane of thickness t and radius c, completely spans the ampulla to block fluid flow [Fig. 2(b)] [3]. Along one wall sit sensory *hair cells*, from which bundles of *stereocilia* (of length $\lambda_H \approx 50\ \mu$m [13]) project into the cupula. Thus cupular deformations displace stereocilia and trigger neural signals.

Basic SCC function is shown in Fig. 2(c). An impulsive angular acceleration $\alpha(t) = \Omega_0 \delta(t - t_a)$, viewed in the rest frame of the canal, gives rise to ballistic endolymph motion with initial angular velocity Ω_0. Viscous resistance from the walls cuts off this inertial motion after a time τ_f ($\sim$5 ms in humans), during which a volume $V_c \propto \Omega_0$ of fluid passes through the canal and distorts the cupula [Fig. 2(c), part (i)]. The elastic restoring force of the distorted cupula drives fluid back through the narrow duct. Viscous resistance from duct walls slows cupular relaxation to a time scale τ_s (4–7 s in humans and primates [14,15]), so that V_c encodes angular velocity Ω for $t \lesssim \tau_s$. Under sustained rotation, however, the cupula relaxes [Fig. 2(c), part (ii)] and "forgets" the constant rotation rate Ω_0. Upon stopping, the sudden deceleration displaces the cupula in the opposite direction [Fig. 2(c), part (iii)], causing dizziness (the false sensation of rotation). The shorter the τ_s, the more quickly an organism becomes dizzy.

Simple arguments give scaling relations for SCC processes. Fluid "knows" that walls are accelerating only after vorticity created at the walls diffuses (with diffusivity $\nu = \mu/\rho$) to the duct center, giving an inertial time $\tau_f \sim d^2/\nu$. During τ_f, fluid moves ballistically with velocity $\Omega_0 R$, so that a fluid volume $V_c \sim (\pi d^2)\Omega_0 R \tau_f$ travels through the duct. Once inertia is cut off, the cupula relaxes quasistatically, as the elastic restoring pressure $\Delta P = K V_c$ drives a Poiseuille flow $\dot{V}_c \sim \Delta P d^4/\mu\beta_d R$, assuming viscous resistance to be dominated in the narrow duct. An ordinary differential equation for V_c results, whose solutions decay exponentially on a time scale $\tau_s \sim \mu\beta_d R/K d^4$.

Prefactors were obtained by solving for the time-dependent flow due to an impulsive acceleration, giving

$$V_c = \frac{4\pi d^4 R\alpha}{\lambda_0^4 \nu}\Omega_0, \qquad \tau_f = \frac{d^2}{\nu\lambda_0^2}, \qquad \tau_s = \frac{8\mu\beta_d R}{K\pi d^4}, \tag{1}$$

where $\lambda_0 \approx 2.4$ is the first zero of the Bessel function J_0, and $\alpha \approx 1.3$ is a geometric factor [16].

The final physical ingredient involves elastic deformations of the cupula, which we treat as a clamped plate of modulus $E_0 = E'(1 - \sigma^2)$ and Poisson ratio σ [17]. A plate of bending rigidity $D_0 = E' t^3/12$ obeys $D_0 \nabla^4 w = \Delta P$, giving a deformed profile $w = w_{\max}[1 - (r/c)^2]^2$, where $w_{\max} = \Delta P c^4/64 D_0$ [18]. Integrating, we obtain the cupular stiffness $K = \Delta P_c/V_c$,

$$K = E' \frac{16}{\pi}\frac{t^3}{c^6}, \tag{2}$$

whose value $K = 4.6\ \mathrm{GPa/m^3}$ is derived using (1) and measured values of $\tau_s \approx 4$ s. This implies $E' \approx 2\ \mathrm{dyn/cm^2}$, consistent with measurements for mucus [19].

Having described the mechanical response, we now connect cupular displacement w to stereociliar tip displacement ζ (and thus to a neural firing rate f). Hair cells have a high resting discharge rate f_r and are bidirectionally sensitive, so that deflections in either direction can be sensed quickly [3]. Within each bundle, stereociliar tips are linked by filamentous "gating springs" that open or close ion channels when the tips are displaced, and f changes linearly with (small) ζ [20]. In other inner-ear organs, hair cells adapt rapidly ($<$100 ms) [20]; SCC hair cell adaptation requires much longer (tens of seconds) [21] and is ignored here. Since the tips are embedded in the cupula, ζ varies with V_c via

$$\zeta \approx \frac{4\lambda_H^2}{c^2} w_{\max} = \frac{12\lambda_H^2}{\pi c^4} V_c \quad \text{for} \quad \lambda_H \ll c. \tag{3}$$

Measurements on 5–10 μm utricular and cochlear hair cells indicate a threshold displacement $\zeta_{\min} \sim \mathcal{O}(\text{nm})$ for neural activity, and gating spring models predict $\zeta_{\min}$ to vary with hair cell length [20]. One expects SCC hair cells, roughly 10 times longer, to have $\zeta_{\min} \sim \mathcal{O}(10\ \text{nm})$. A similar value can be obtained in another fashion: Physiological measurements indicate a lower limit $\Omega_{\min} \approx 2^\circ/\text{s}$ for sensation in humans [22], which implies

$$\zeta_{\min} \approx 20\ \text{nm} \tag{4}$$

using (1) and (3). An upper limit on measurable rotation comes from natural firing rate limits: f must be positive but below a maximum (injured) rate ~400 Hz. In squirrel monkeys, $\Delta f \approx \alpha\Omega$, where $\alpha \approx 0.24/^\circ$ [15]. Zeroing deflections ζ_{sat} occur for $\Delta f \sim f_r \approx 100$ Hz, implying a "zeroing" rotation $\Omega_{\text{zero}} = f_r/\alpha \approx 420^\circ/\text{s}$, giving $\zeta_{\text{zero}} \approx 4$ μm. As expected, this is about 10 times larger than ζ_{zero} measured for utriclar hair cells [23].

The sensitivity S of an SCC follows from (1) and (3), with minimum detectable rotation $\Omega_{\min}$,

$$\Omega_{\min} = \frac{\lambda_0^4 \mu}{48\lambda_H^2 \alpha}\frac{c^4}{d^4 R}\zeta_{\min} \equiv S^{-1}\zeta_{\min}. \tag{5}$$

We have now characterized the mechanical-neural signal transduction process and can examine the effect of varying SCC dimensions. We scale SCC variables by their human values, denote scaled variables with hats, and pose the central question: Given blueprints (Fig. 2) and basic building materials (μ, ρ, E', λ_H, $\zeta_{\min}$, and ζ_{sat}), what dimensions $\{\hat{R}, \hat{c}, \hat{d}, \hat{t}\}$ maximize SCC sensitivity $\hat{S} = \hat{d}^4\hat{R}/\hat{c}^4$?

Certain constraints, however, must be obeyed for a physically and a physiologically viable SCC. First, thermal fluctuations of the cupula must be small enough to escape detection, or else balance and vision would be impaired. The probability of a cupular displacement fluctuation V_c is given by $P(V_c) \sim \exp(-KV_c^2/2k_BT)$. We use (2) and (3) to express $P(V_c)$ in terms of ζ, giving $P(\zeta) = 2\sqrt{\sigma/\pi}\exp(-\sigma\zeta^2)$, where $\sigma = \pi E' c^2 t^3/18 k_B T \lambda_H^4$. The probability of sensing a thermal fluctuation is given by $P(\zeta > \zeta_{\min}) = 1 - \text{erf}(\sigma^{1/2}\zeta_{\min})$. Requiring $P(\zeta > \zeta_{\min})$ to be smaller than some value $\epsilon = 10^{-5}$ gives

$$\hat{c}^{\,2/3}\hat{t} > \left(9.7\frac{18\lambda_h^4 k_B T}{\pi E' \zeta_{\min}^2 c_h^2 t_h^3}\right)^{1/3} \equiv A = 0.15. \tag{6}$$

Note that A is rather insensitive to ϵ: $A(10^{-6}) = 0.16$ and $A(10^{-4}) = 0.14$.

Second, the cupula should encode angular *velocity* for as long as possible. The smaller the τ_s, the sooner angular velocity is "forgotten" and dizziness ensues. Requiring τ_s to be larger than some minimum time τ_s^m gives

$$\frac{\hat{R}\hat{c}^6}{\hat{d}^4\hat{t}^3} > \frac{2E'\tau_s^m}{\mu\beta_d}\frac{t_h^3 d_h^4}{R_h c_h^6} \equiv B = 0.25, \tag{7}$$

and we take $\tau_s^m = 1$ s as a basic estimate.

Third, the maximum cupular deflection $w_{\max}$ for physiological rotations should be small (compared to t), to avoid damaging the cupula and for a linear response. The zeroing rotation Ω_{zero} is one example, giving

$$\frac{\hat{c}^2}{\hat{t}} < \frac{4\lambda_h^2}{\zeta_{\text{zero}}}\frac{t_h}{c_h^2} \equiv C = 4.1. \tag{8}$$

Rotations $\Omega_{\max}$ which zero the neural signal, but may still be physiologically relevant, also impose a constraint. As a basic estimate, we take $\Omega_{\max} = 2\pi$ rad/s, which gives

$$\frac{\hat{d}^4\hat{R}}{\hat{c}^2\hat{t}} < \frac{\lambda_0^4\nu}{12\alpha\Omega_{\max}}\frac{c_h^2 t_h}{d_h^4 R_h} \equiv D = 4.5. \tag{9}$$

Finally, the ampulla must fit in the canal,

$$\hat{R}/\hat{c} > 2c_h/R_h \equiv E = 0.32, \tag{10}$$

and the cupula should be platelike for uniform ζ,

$$\hat{c}/\hat{t} > t_h/c_h \equiv F = 0.70. \tag{11}$$

Constraints (6)–(11) restrict parameter space significantly (Fig. 3).

Equations (5)–(11) represent a nonlinear multidimensional optimization, but an equivalent linear optimization is obtained by taking the logarithm of each equation. As in linear programming, extrema are found at vertices of the constraint equations (or $-\infty$, since logs can be negative). Here, the most sensitive SCC geometry is found at vertices A, B, D, and F, giving dimensions

$$\hat{R} = \frac{(BD)^{1/2}}{F^2} = 2.1, \qquad \hat{c} = (AF)^{3/5} = 0.26, \tag{12}$$

$$\hat{d} = \frac{A^{9/20}D^{1/8}F^{7/10}}{B^{1/8}} = 0.49, \qquad \hat{t} = \frac{A^{3/5}}{F^{2/5}} = 0.38, \tag{13}$$

and a sensitivity $\hat{S}$,

$$\hat{S} = DA^{-3/5}F^{-8/5} \approx 24, \tag{14}$$

that is about 24 times greater than the human SCC. As seen in Fig. 1, these dimensions compare quite favorably with available data—particularly since such an optimum need not exist in the first place, and, even if it did, its dimensions could have differed from those found in nature by many orders of magnitude.

Two parameters ($\Omega_{\max}$ and τ_s^m) were chosen somewhat arbitrarily, and it is natural to question how these choices affect the above results. Only $\hat{R}$ and $\hat{d}$ depend on these choices, but weakly: $\hat{R} \sim (\tau_s^m/\Omega_{\max})^{1/2}$ and $\hat{d} \sim (\tau_s^m\Omega_{\max})^{-1/8}$. For $\hat{R}$ to change by an order of magnitude, $\tau_s^m/\Omega_{\max}$ must be off by two, so the optimum is robust and insensitive to these crude choices. Variations in τ_s^m and $\Omega_{\max}$ across species would lead to only slight differences in optimal SCC dimensions; such variations could perhaps explain the slight slopes in Fig. 1. For example, "physiological" rotation rates (and thus $\Omega_{\max}$) almost certainly decrease with organism size, giving optimal R and d that increase slightly with mass.

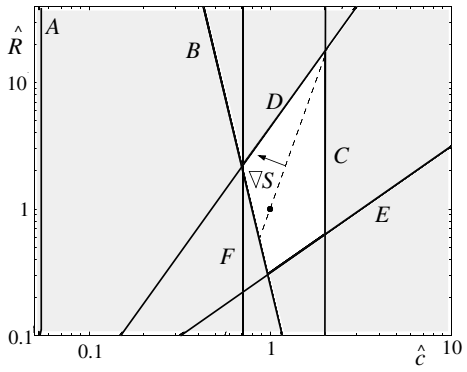

FIG. 3. A 2D slice of 4D parameter space showing the constrained space available for viable SCC design. Constraints (6)–(11) are labeled *A*–*F*. Also plotted is the sensitivity gradient and, for reference, human SCC dimensions. The optimal SCC is found at the vertex of constraints *A*, *B*, *D*, and *F*.

While the above analysis assumes perfect "machine tools," nature's machinery has a rather larger tolerance: variations in human SCC dimension are of order 10% [24]. To allow for imperfect "machining," we find the most sensitive "tolerant" SCC such that 10% variations in any dimension satisfy constraints *A*–*F*, giving

$$\hat{R} = 1.9, \quad \hat{c} = 0.33, \quad \hat{d} = 0.46, \quad \hat{t} = 0.38, \quad (15)$$

with a relative sensitivity $\hat{S} \approx 7$. SCC sensitivity variations due to size variations range from about 0.4 to 2.5 times that of the "average" canal.

No constraint on measurement time τ_f was introduced, although it plays an important role in vision: to be "watched," an image must be kept within one retinal fovea—about 1° in humans [3]. In the time τ_f following an Ω_0 impulse, the eye/fovea lags the image by $\Delta\theta \sim \Omega_0\tau_f$, so that the maximum rotation allowing a fixed gaze is $\Omega_v \sim 1°/\tau_f \sim 200°/\mathrm{s}$. If a larger Ω_v were required, d would be further constrained.

Although we have explicitly discussed mammals, the same SCC dimensions are found in all vertebrates, with a few notable exceptions. Head size is an obvious and unavoidable constraint for exceedingly small fish larvae, whose SCCs start small and grow with the fish [7]. As a group, sharks (even small ones) have abnormally large SCCs ($R \sim 40$ mm) [7]. Since sharks broke from other vertebrates quite early in evolution, perhaps differences in building materials (E or hair cell properties) exist.

In summary, we have argued that evolution has converged on an optimal design for a maximally sensitive rotation detector. The optimal SCC is well constrained, with little room for variations, and falls within a factor of 5 of available data. The optimum itself is robust and depends on basic mechanics and established hair cell properties; the "calibrating" assumptions made herein are self-consistent, but not essential for this central result. It would be interesting to see whether this approach will be useful in understanding other biological systems.

I am grateful to Howard Stone for introducing me to the vestibular system and for many discussions, and to Michael Brenner for early conversations about optimization. Conversations with Bill Bialek, Eric Lauga, and Larry Hoffman are gratefully acknowledged.

[1] S. Vogel, *Life's Devices* (Princeton University Press, Princeton, 1988); Phys. Today **51**, No. 11, 22 (1998); T. A. McMahon and J. T. Bonner, *On Size and Life* (Scientific American Library, New York, 1983).
[2] A. W. Gummer, *Biophysics of the Cochlea* (World Scientific, Singapore, 2003); T. Duke and F. Julicher, Phys. Rev. Lett. **90**, 158101 (2003).
[3] R. L. Lewis, E. L. Leverenz, and W. S. Bialek, *The Vertebrate Inner Ear* (CRC Press, Boca Raton, 1985).
[4] D. E. Parker, Sci. Am. **243**, 118 (1980).
[5] T. M. Squires, M. S. Weidman, T. C. Hain, and H. A. Stone, J. Biomech. **37**, 1137 (2004).
[6] G. M. Jones and K. E. Spells, Proc. R. Soc. London B **157**, 403 (1963); J. H. Ten Kate, J. W. Kuiper, and H. H. van Barnevald, J. Exp. Biol. **53**, 501 (1970).
[7] M. Muller, J. Theor. Biol. **198**, 405 (1999).
[8] T. Hoshino, Acta Oto-Laryngol. **93**, 349 (1982).
[9] J. Aizenberg, A. Tkachenko, S. Weiner, L. Addadi, and G. Hendler, Nature (London) **412**, 819 (2001).
[10] V. C. Sundar, A. D. Yablon, J. L. Grazul, M. Ilan, and J. Aizenberg, Nature (London) **424**, 899 (2003).
[11] D. A. Baylor, T. D. Lamb, and K. W. Yau, J. Physiol. (London) **288**, 613 (1979).
[12] W. Denk and W. W. Webb, Phys. Rev. Lett. **63**, 207 (1989).
[13] D. E. Hillman, Prog. Brain Res. **37**, 69 (1972).
[14] M. J. Dai, A. Klein, B. Cohen, and T. Raphan, J. Vestibular Res. **9**, 293 (1999).
[15] J. M. Goldberg and C. Fernandez, J. Neurophysiol. **34**, 635 (1971).
[16] W. C. Van Buskirk, R. G. Watts, and Y. K. Liu, J. Fluid Mech. **78**, 87 (1976).
[17] R. D. Rabbitt and E. R. Damiano, J. Fluid Mech. **238**, 337 (1992).
[18] L. D. Landau and E. M. Lifshitz, *Theory of Elasticity* (Butterworth-Heinemann, Oxford, 2000).
[19] M. King and P. T. Macklem, J. Appl. Physiol. **42**, 797 (1977).
[20] V. S. Markin and A. J. Hudspeth, Annu. Rev. Biophys. Biomol. Struct. **24**, 59 (1995); A. J. Hudspeth and V. S. Markin, Phys. Today **47**, No. 2, 22 (1994).
[21] S. Masetto, P. Perin, L. Botta, G. Zucca, and P. Valli, Neuroreport. **7**, 230 (1995).
[22] C. M. Oman and L. R. Young, Acta Oto-Laryngol. **74**, 324 (1972).
[23] A. J. Hudspeth and D. P. Corey, Proc. Nat. Acad. Sci. U.S.A. **74**, 2407 (1977).
[24] I. S. Curthoys and C. M. Oman, Acta Oto-Laryngol. **103**, 254 (1987).
[25] Animal c and t are generally unavailable, so we measured the photographs of A. A. Gray, *The Labyrinth of Animals* (Churchill, London, 1907). Cupula thickness was based on crista width, when unambiguous.